



# Nuclear Pasta in Cold Non-Accreting Neutron Stars: Symmetry Energy Effects <sup>†</sup>

Nikolai N. Shchepochin <sup>1,\*</sup>, John M. Pearson <sup>2</sup> and Nicolas Chamel <sup>1</sup>

<sup>1</sup> Institut d’Astronomie et d’Astrophysique, CP-226, Université Libre de Bruxelles, 1050 Brussels, Belgium; e-mail@e-mail.com

<sup>2</sup> Dépt. de Physique, Université de Montréal, Montréal, QC H3C 3J7, Canada; e-mail@e-mail.com

\* Correspondence: nikolai.shchepochin@ulb.be

<sup>†</sup> Presented at the 2nd Electronic Conference on Universe, 16 February–2 March 2023; Available online: <https://ecu2023.sciforum.net/>.

**Abstract:** The densest part of neutron star crusts may contain very exotic nuclear configurations, so-called nuclear pasta. We investigate the effect of nuclear symmetry energy on the existence of such phases in cold non-accreting neutron stars. For this purpose, we apply three Brussel-Montreal functionals based on generalized Skyrme effective interactions, whose parameters were accurately calibrated to reproduce both experimental data on nuclei and realistic neutron-matter equations of state. These functionals differ in their predictions for the density dependence of the symmetry energy. Within the fourth-order extended Thomas-Fermi method, we find that pasta occupies a wider region of the crust for models with a lower slope of the symmetry energy (and higher symmetry energy at relevant densities) in agreement with previous studies based on pure Thomas-Fermi approximation and compressible liquid-drop models. However, the incorporation of microscopic corrections consistently calculated with the Strutinsky integral method leads to a significant shift of the onset of the pasta phases to higher densities due to the enhanced stability of spherical clusters. As a result, the pasta region shrinks substantially, and the role of symmetry energy weakens. This study sheds light on the importance of quantum effects for reliably describing pasta phases in neutron stars.

**Keywords:** neutron stars; equation of state; dense matter structure

## 1. Introduction

The region between the liquid core and the solid crust of neutron stars (NS) may consist of very exotic matter phases in which nuclei adopt unusual pasta-like shapes. Such configurations were first predicted within compressible liquid drop models (CLDMs) [1,2] (see [3,4] for recent studies) and later investigated in more microscopic frameworks [5–11]. Due to the different arrangement of nucleons, pasta phases can affect the properties of the NS crust [12–14] and manifest themselves in astrophysical observations [15–17].

However, the abundance of pasta phases varies in different applied nuclear models and, in particular, depends on the symmetry energy. The latter is defined as the difference between pure neutron matter (NeuM) and symmetric nuclear matter (SNM) and can be expanded near the saturation density,  $n_0 \approx 0.16 \text{ fm}^{-3}$ , as:

$$S(n) = e_{\text{NeuM}} - e_{\text{SNM}} = \tilde{J} + \frac{1}{3} \tilde{L} \varepsilon + \frac{1}{18} \tilde{K}_{\text{sym}} \varepsilon^2 + \dots, \quad (1)$$

where  $\varepsilon = (n - n_0)/n_0$ .  $\tilde{J}$ ,  $\tilde{L}$  and  $\tilde{K}_{\text{sym}}$  are the symmetry energy coefficient, its slope and curvature, respectively. In Figure 1, we have plotted the symmetry energy as a function of the baryon density for our generalized Skyrme effective interactions of the BSk family

**Citation:** Shchepochin, N.N.; Pearson, J.M.; Chamel, N. Nuclear Pasta in Cold Non-Accreting Neutron Stars: Symmetry Energy Effects. *Phys. Sci. Forum* **2023**, *3*, x.

<https://doi.org/10.3390/xxxxx>

Published: 15 February 2023



**Copyright:** © 2023 by the authors. Submitted for possible open access publication under the terms and conditions of the Creative Commons Attribution (CC BY) license (<https://creativecommons.org/licenses/by/4.0/>).

[18]. BSk22, BSk24, and BSk25 were fitted to the same data (experimental atomic masses of [19] and NeuM equation of state (EoS) of [20]) but for different values of  $\tilde{J}$ . These functionals exhibit different behaviours for  $S(n)$ , which can be conveniently described by the slope  $\tilde{L}$ . Namely the lower  $\tilde{L}$  leads to higher values of the symmetry energy  $S(n)$  at  $n \lesssim 0.11 \text{ fm}^{-3}$ . Therefore, one can use these functionals to study the symmetry energy effects.

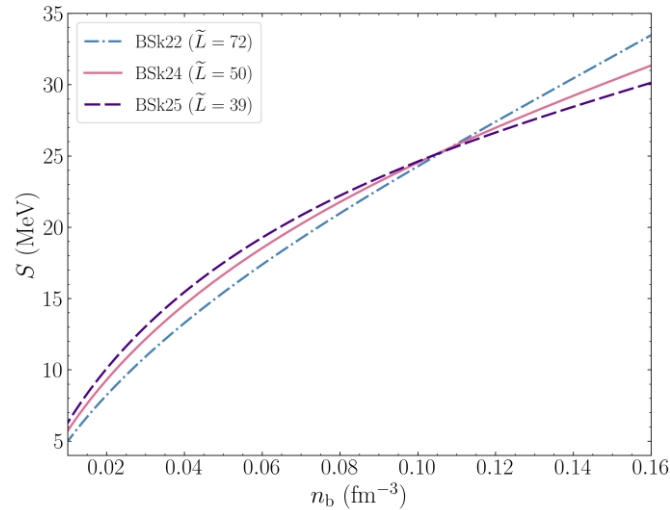


**Figure 1.** Symmetry energy as a function of the baryon density for BSk functionals [18].

The influence of the symmetry energy on the presence of pasta phases in NS was previously investigated within CLDMs [3,4] and Thomas-Fermi (TF) approximation [5–7]. The main conclusion was that the abundance of pasta increases with decreasing  $\tilde{L}$ . However, such (semi-)classical models lack important microscopic features such as shell structure and pairing. These effects are naturally taken into account in self-consistent mean-field calculations, but such computations are generally restricted to fixed proton fractions  $Y_p$ , see, e.g., [10], rather than  $\beta$ -equilibrium because of their very high computational cost. For this reason, we have applied the fourth-order extended Thomas-Fermi (ETF) method [21] and incorporated quantum corrections perturbatively [22–24] to study the role of the symmetry energy on pasta.

## 2. Methods

To determine the equilibrium nuclear matter shape, we minimize the energy per nucleon for each kind of pasta configuration: sphere, spaghetti, lasagna, bucatini and Swiss cheese. We start from the semi-classical calculations, where the fourth-order ETF energy (omitting the neutron mass energy contribution by convention) can be written as:

$$e_{\text{ETF}} = e_{\text{nuc}} + e_c + e_e - Y_p Q_{n,\beta}. \quad (2)$$

Here  $e_{\text{nuc}}$  represents the nuclear energy. The second and third terms account for the Coulomb and electron contributions respectively [9,24].  $Q_{n,\beta}$  is the neutron  $\beta$ -decay energy.

For the functionals adopted here, the nuclear energy depends on the local number density  $n_q(\mathbf{r})$ , kinetic energy-density  $\tau_q(\mathbf{r})$  and spin-orbit current density  $J_q(\mathbf{r})$  at position  $\mathbf{r}$ , where  $q = n, p$ . Within the ETF approximation  $\tau_q$  and  $J_q$  can be expanded in terms of  $n_q$  and its derivatives (see [21,22]), then:

$$e_{\text{nuc}} = \frac{1}{A} \int \mathcal{E}_{\text{Sky}}(\mathbf{r}) d^3\mathbf{r}, \quad (3)$$

where the integration is performed over the Wigner-Seitz cell containing  $A$  nucleons and  $\mathcal{E}_{\text{Sky}}$  is the local nuclear energy density obtained from generalized Skyrme effective interactions [25]. We use the parametrization of [22] for the number density profiles, which allows for simplifications of the fourth-order ETF expressions.

In a second step, we implement quantum corrections for protons via the Strutinsky integral theorem [22,26] if the protons are bound in the clusters at least in one direction (their Fermi energy is lower than their mean field potential at the cell border). We also take pairing into account through the local density approximation [26]. The final expression for the ETFSIp energy is obtained by adding these two corrections. We then vary the number of protons in the cell to find the optimal value.

### 3. Results and Discussion

To visualize our results, we display in Figure 2 colour bars corresponding to the sequence of pasta phases for functionals of the BSk family, as predicted by the pure ETF calculations and after adding the quantum corrections.

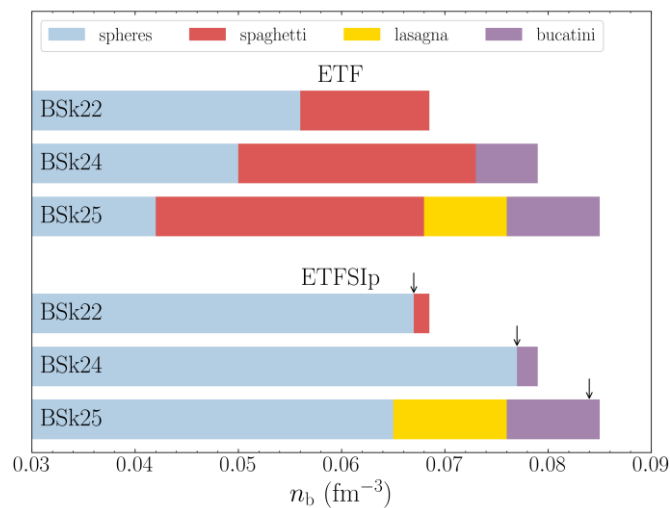


**Figure 2.** Horizontal bars illustrate the different phases of NS crusts as a function of the baryon density. Blue regions are for spheres, red for spaghetti, yellow for lasagna and purple for bucatini. Arrows denote the onset of proton drip for spheres. Results are obtained in ETF and ETFSIp approaches for three BSk functionals [18].

Within the ETF approach, pasta structures appear at a high enough density for all considered functionals. The widest diversity of pasta shapes is found for the BSk25 functional, for which all types are present except for Swiss cheese. This stems from the fact that this functional exhibits the lowest slope of the symmetry energy. Specifically, one can notice that among the considered BSk series, a lower  $\tilde{L}$  leads to a lower threshold density for the onset of the pasta phases and a larger density,  $n_{\text{cc}}$ , for the crust-core transition (the latter correlation is also found when the crust is supposed to contain only spherical clusters [27]). Therefore, within the ETF approach, a lower slope  $\tilde{L}$  implies that the region filled with pasta spans a larger range of density.

When quantum corrections are added on top of the ETF energy, pasta phases almost disappear. This, in particular, is caused by the fact that the spaghetti phase occurs to be strongly energetically unfavored. This phase persists only for the BSk22 functional beyond proton drip (marked by arrows) because the Strutinsky integral correction is then dropped. Since proton drip occurs at density below the crust-core transition, the correlation between  $\tilde{L}$  and  $n_{\text{cc}}$  holds. However, the overall influence of  $\tilde{L}$  on the pasta abundance is blurred since for the BSk22, BSk24 pasta is confined to very small density domains.

#### 4. Conclusions

In this paper, we have extended our previous work [26], where pasta phases were calculated within the fourth-order ETF method with quantum corrections added perturbatively. Namely, we have performed calculations with two more parametrizations of generalized Skyrme effective interactions, which differ in the symmetry energy behaviour (see Figure 1) to study its role. Within the semi-classical ETF approach, we found that the density domain consisting of pasta phases is larger for the functionals with a lower slope of the symmetry energy  $\tilde{L}$ . Such a conclusion is likely to be connected with more favoured clustering for low  $\tilde{L}$  and is in agreement with previous works [3–7].

However, when quantum corrections are included, the stability of spherical clusters increases so that the pasta region significantly shrinks. This is also due to the partial elimination of the spaghetti phase. Although for the BSk25 functional with the lowest  $\tilde{L}$  the pasta abundance still remains the largest among the considered functionals, the effects of quantum corrections outweigh those of the symmetry energy for the two other functionals, for which pasta phases appear only beyond proton drip where the quantum corrections are dropped and occupy almost equally small density domain independently of  $\tilde{L}$ . Therefore, quantum corrections can play a more important role than symmetry energy. This calls for fully self-consistent mean-field calculations in future works.

**Author Contributions:** Calculations, original draft preparation, N.N.S.; conceptualization, supervision, J.M.P. and N.C. All authors have read and agreed to the published version of the manuscript.

**Funding:** This work was financially supported by F.R.S.-FNRS (Belgium) under Grant No. IISN 4.4502.19. It has also received funding from the FWO (Belgium) and the F.R.S.-FNRS (Belgium) under the Excellence of Science (EOS) programme (project No. 40007501).

**Institutional Review Board Statement:**

**Informed Consent Statement:** Not applicable.

**Data Availability Statement:** Data are available upon reasonable request.

**Conflicts of Interest:** The authors declare no conflict of interest.

#### References

1. Ravenhall, D.G.; Pethick, C.J.; Wilson, J.R. Structure of Matter below Nuclear Saturation Density. *Phys. Rev. Lett.* **1983**, *50*, 2066–2069. <https://doi.org/10.1103/PhysRevLett.50.2066>.
2. Hashimoto, M.; Seki, H.; Yamada, M. Shape of nuclei in the crust of a neutron star. *Prog. Theor. Phys.* **1984**, *71*, 320–326. <https://doi.org/10.1143/PTP.71.320>.
3. Dinh Thi, H.; Fantina, A.F.; Gulminelli, F. The effect of the energy functional on the pasta-phase properties of catalysed neutron stars. *Eur. Phys. J. A* **2021**, *57*, 296. <https://doi.org/10.1140/epja/s10050-021-00605-6>.
4. Newton, W.G.; Gearheart, M.; Li, B.A. A Survey of the Parameter Space of the Compressible Liquid Drop Model as Applied to the Neutron Star Inner Crust. *Astrophys. J. Suppl. Ser.* **2013**, *204*, 9. <https://doi.org/10.1088/0067-0049/204/1/9>.
5. Oyamatsu, K.; Iida, K. Symmetry energy at subnuclear densities and nuclei in neutron star crusts. *Phys. Rev. C* **2007**, *75*, 015801. <https://doi.org/10.1103/PhysRevC.75.015801>.
6. Grill, F.; Providência, C.; Avancini, S.S. Neutron star inner crust and symmetry energy. *Phys. Rev. C* **2012**, *85*, 055808. <https://doi.org/10.1103/PhysRevC.85.055808>.
7. Bao, S.S.; Shen, H. Impact of the symmetry energy on nuclear pasta phases and crust-core transition in neutron stars. *Phys. Rev. C* **2015**, *91*, 015807. <https://doi.org/10.1103/PhysRevC.91.015807>.
8. Shchepochin, N.N.; Zemlyakov, N.A.; Chugunov, A.I.; Gusakov, M.E. Pasta Phases in Neutron Star Mantle: Extended Thomas–Fermi vs. Compressible Liquid Drop Approaches. *Universe* **2022**, *8*, 582. <https://doi.org/10.3390/universe8110582>.
9. Pearson, J.M.; Chamel, N.; Potekhin, A.Y. Unified equations of state for cold nonaccreting neutron stars with Brussels–Montreal functionals. II. Pasta phases in semiclassical approximation. *Phys. Rev. C* **2020**, *101*, 015802. <https://doi.org/10.1103/PhysRevC.101.015802>.
10. Fattoyev, F.J.; Horowitz, C.J.; Schuetrumpf, B. Quantum nuclear pasta and nuclear symmetry energy. *Phys. Rev. C* **2017**, *95*, 055804. <https://doi.org/10.1103/PhysRevC.95.055804>.
11. Gögelein, P.; Muther, H. Nuclear matter in the crust of neutron stars. *Phys. Rev. C* **2007**, *76*, 024312. <https://doi.org/10.1103/PhysRevC.76.024312>.

12. Pethick, C.J.; Potekhin, A.Y. Liquid crystals in the mantles of neutron stars. *Phys. Lett. B* **1998**, *427*, 7–12. [https://doi.org/10.1016/S0370-2693\(98\)00341-4](https://doi.org/10.1016/S0370-2693(98)00341-4).
13. Yakovlev, D.G. Electron transport through nuclear pasta in magnetized neutron stars. *Mon. Not. R. Astron. Soc.* **2015**, *453*, 581–590. <https://doi.org/10.1093/mnras/stv1642>.
14. Caplan, M.E.; Horowitz, C.J. Colloquium: Astromaterial science and nuclear pasta. *Rev. Mod. Phys.* **2017**, *89*, 041002. <https://doi.org/10.1103/RevModPhys.89.041002>.
15. Horowitz, C.J.; Berry, D.K.; Briggs, C.M.; Caplan, M.E.; Cumming, A.; Schneider, A.S. Disordered Nuclear Pasta, Magnetic Field Decay, and Crust Cooling in Neutron Stars. *Phys. Rev. Lett.* **2015**, *114*, 031102. <https://doi.org/10.1103/PhysRevLett.114.031102>.
16. Pons, J.A.; Viganò, D.; Rea, N. A highly resistive layer within the crust of X-ray pulsars limits their spin periods. *Nat. Phys.* **2013**, *9*, 431–434. <https://doi.org/10.1038/nphys2640>.
17. Gearheart, M.; Newton, W.G.; Hooker, J.; Li, B.A. Upper limits on the observational effects of nuclear pasta in neutron stars. *Mon. Not. R. Astron. Soc.* **2011**, *418*, 2343–2349. <https://doi.org/10.1111/j.1365-2966.2011.19628.x>.
18. Goriely, S.; Chamel, N.; Pearson, J.M. Further explorations of Skyrme-Hartree-Fock-Bogoliubov mass formulas. XIII. The 2012 atomic mass evaluation and the symmetry coefficient. *Phys. Rev. C* **2013**, *88*, 024308. <https://doi.org/10.1103/PhysRevC.88.024308>.
19. Audi, G.; Meng, W.; Wapstra, A.; Kondev, F.; MacCormick, M.; Xu, X.; Pfeiffer, B. The Ame2012 atomic mass evaluation. *Chin. Phys. C* **2012**, *36*, 1287. <https://doi.org/10.1088/1674-1137/36/12/002>.
20. Li, Z.H.; Schulze, H.J. Neutron star structure with modern nucleonic three-body forces. *Phys. Rev. C* **2008**, *78*, 028801. <https://doi.org/10.1103/PhysRevC.78.028801>.
21. Brack, M.; Guet, C.; Håkansson, H.B. Selfconsistent semiclassical description of average nuclear properties—A link between microscopic and macroscopic models. *Phys. Rep.* **1985**, *123*, 275–364. [https://doi.org/10.1016/0370-1573\(86\)90078-5](https://doi.org/10.1016/0370-1573(86)90078-5).
22. Onsi, M.; Dutta, A.K.; Chatri, H.; Goriely, S.; Chamel, N.; Pearson, J.M. Semi-classical equation of state and specific-heat expressions with proton shell corrections for the inner crust of a neutron star. *Phys. Rev. C* **2008**, *77*, 065805. <https://doi.org/10.1103/PhysRevC.77.065805>.
23. Pearson, J.M.; Chamel, N.; Pastore, A.; Goriely, S. Role of proton pairing in a semimicroscopic treatment of the inner crust of neutron stars. *Phys. Rev. C* **2015**, *91*, 018801. <https://doi.org/10.1103/PhysRevC.91.018801>.
24. Pearson, J.M.; Chamel, N.; Potekhin, A.Y.; Fantina, A.F.; Ducoin, C.; Dutta, A.K.; Goriely, S. Unified equations of state for cold non-accreting neutron stars with Brussels-Montreal functionals—I. Role of symmetry energy. *Mon. Not. R. Astron. Soc.* **2018**, *481*, 2994–3026. <https://doi.org/10.1093/mnras/sty2413>.
25. Chamel, N.; Goriely, S.; Pearson, J.M. Further explorations of Skyrme-Hartree-Fock-Bogoliubov mass formulas. XI Stabilizing neutron stars against a ferromagnetic collapse. *Phys. Rev. C* **2009**, *80*, 065804. <https://doi.org/10.1103/PhysRevC.80.065804>.
26. Pearson, J.M.; Chamel, N. Unified equations of state for cold nonaccreting neutron stars with Brussels-Montreal functionals. III. Inclusion of microscopic corrections to pasta phases. *Phys. Rev. C* **2022**, *105*, 015803. <https://doi.org/10.1103/PhysRevC.105.015803>.
27. Ducoin, C.; Margueron, J.; Providência, C. Nuclear symmetry energy and core-crust transition in neutron stars: A critical study. *Europhys. Lett.* **2010**, *91*, 32001. <https://doi.org/10.1209/0295-5075/91/32001>.

**Disclaimer/Publisher’s Note:** The statements, opinions and data contained in all publications are solely those of the individual author(s) and contributor(s) and not of MDPI and/or the editor(s). MDPI and/or the editor(s) disclaim responsibility for any injury to people or property resulting from any ideas, methods, instructions or products referred to in the content.